Surface free energy of zirconia crowns after airborne-particle abrasion

***Arne Sebastian Rossow**, Dental student **
***Susanna Patiño Walbækken**, Dental student **

*Hanna Tiainen, PhD, Associate professor * Department of Biomaterial Science*
*Hans Jacob Rønold, Dr. odont, Associate professor, Prosthodontist * Department of Prosthetic Dentistry and Oral Function*
*Lars-Fredrik Gjølstad, Cand. odont, Clinical Spesialist, Prosthodontist **

** Institute of Clinical Dentistry, Faculty of Dentistry, University of Oslo*

UiO : Det odontologiske fakultet

Susanna Patiño Walbækken
Arne Sebastian Rossow

Content

Susanna Patiño Walbækken
Arne Sebastian Rossow

1. Introduction

Zirconia (ZrO_2) has in recent years become a popular dental crown material due to its good esthetic and biomechanical properties. (1) There are many different types of zirconia materials with different biomechanical properties as well as esthetic properties. Often are different zirconia materials used in the same crown to gain optimal esthetical properties. (2) (3)

Zirconia is a polymorphic material that appears in different crystal forms at different temperatures; monoclinic, tetragonal, or cubic. (4) A change in temperature, increased humidity, and increased stress can affect the zirconia and make it undergo a phase transformation from tetragonal to monoclinal phase. This will result in expansion of the material (3-4%), as the lattice structure of the tetragonal phase is denser than in the monoclinal phase. (5) To prevent the uncontrolled phase transformation from tetragonal to monoclinic and the associated volume expansion upon cooling of sintered zirconia, yttrium is added (3 mol.%) to stabilize zirconia in tetragonal form. (6) The reason for preventing volume expansion, is because the material becomes very brittle and the forces induced during changes between the phases result in crack formation, therefore making it not suited as a dental material. (7) (5)

The different zirconia materials used are dependent on the yttrium concentration. We can roughly divide them into three generations of zirconia. (8) The first generation consists of opaque zirconia material, stabilized with 3 mol.% yttrium. This opaque appearance is due to the large intergranular alumina (Al_2O_3) grain size. Alumina is added because it is effective at suppressing the hydrothermal degradation when sintering. (9) The second generation of dental zirconia drastically reduced the concentration of the alumina additive, as well as more evenly distributed Al_2O_3 content and smaller grain size. By also raising the sintering temperature, the porosities in the material were eliminated, making the second generation more translucent than the first generation. (10) The third-generation zirconia is a highly translucent material. When adding 4-5 mol.% yttrium, large amount of the zirconia crystals will be stabilized in cubic phase, which is more translucent, as the light penetrates deeper into the material because of the cubic lattice structure. (11) 3rd generation zirconia is therefore considered to have better esthetic properties. But strength and toughness are diminished because cubic zirconia does not undergo stress-induced phase transformation. (12) The question with the 3rd generation of zirconia is if the material has the same mechanical properties, as well as surface properties, as the 1st and 2nd generation of zirconia. In this study, we want to enlighten any differences between the surface properties of the 2nd and 3rd generation of zirconia. A comparison between these two generations mechanical properties and clinical indications can be seen in Table 1. As seen in Table 1, the biggest differences between 2nd and 3rd generations are the mechanical properties flexural strength and fracture toughness. These properties are the ones that usually determine and play the biggest part on the choice of clinical use.

Table 1: Properties of different zirconia materials. (The values are from (1) and limited data sheet information)

Zirconia material	Some commercial examples	Flexural strength (MPa)	Fracture toughness (MPa $m^{1/2}$)	Translucency parameter (TP) after polishing*	Clinical indications
Translucent zirconia	*Prettau (Zirkonzahn)* *Bruxzir Zirconia (Glidewell Laboratories)* *Wieland Zenostar translucent (Ivoclar Vivadent)*	*≈ 750–1200*	*4–9*	*11.1–13.0*	*Monolithic single crowns or FDPs on teeth and implants with or without veneering of labial facades*
High-translucent zirconia	*Prettau Anterior (Zirkonzahn)* *Katana High translucent (Kuraray Noritake INC)*	*≈ 650–750*	*3–5*	*13.4–15.0*	*Monolithic single crowns or FDPs on teeth and implants with or without veneering of labial facades*

*The translucency parameter is measured from 1 mm thick specimens.

The biggest downside with zirconia, compared to other materials used in fixed dental restorations, is the difficulty in achieving suitable adhesion. (13) Zirconia does not have a glass phase, as opposed to glass ceramics, that can be etched with hydrofluoric acid to increase the surface roughness, as well as chemically bond with a coupling agent (silane). (14) This then affects the clinical indications and possible use of zirconia crowns with certain implications. For optimal bonding between zirconia and the cement, different luting agents are used. Primers containing 10-methacryloyloxydecyl dihydrogen phosphate (10-MDP) have shown good bonding to zirconia, according to a study by Nagaoka et al. (15) This study showed that deprotonated 10-MDP makes ionic interactions with partially positive Zr. Also, 10-MDP has the ability to create hydrogen bonds between P=O and Zr-OH groups, strengthening the bonding between interfaces. (15)

Some commonly used primers, Clearfil Ceramic Primer (Kuraray Noritake, Tokyo, Japan) and Monobond Plus (Ivoclar Vivadent, Schaan, Liechtenstein) contain a silane bi-functional molecule. The effects of silane are unknown in the bonding of zirconia. (16) In this study, we want to look at the differences in surface properties between non-silane primers specified for zirconia (Z-prime plus (17)) compared to the universal primers containing silane (Clearfil Ceramic Primer (18) and Monobond Plus (19)) that are also used with other dental restoration materials, and further investigate how these interact with both generations (2^{nd} and 3^{rd}) of contemporary zirconia material.

A meta-analysis by Inokoshi et al. compares the effectiveness of different treatments to improve bonding strength between zirconia and adhesive cements (16). This meta-analysis suggests that a pretreatment with Al_2O_3 sandblasting, ceramic coating or silica coating is favorable for bonding strength compared to the use of chemical etching, laser irradiation or no mechanical pretreatment. This study also showed a positive effect on the bonding strength by using primers containing 10-MDP.

Micromechanical roughening of the zirconia is used to achieve a better bond. (20) This is done with airborne-particle abrasion (APA) with alumina and gives the zirconia a higher surface area that results in more micromechanical retention. The most commonly used parameters for airborne-particle abrasion are 50 μm Al_2O_3 at 2,5 bar at approximately 10 mm distance from the surface. (21) To consider that the novel aesthetic cubic zirconia materials might be used for bonding procedures other than flat-to-flat (as in resin bonded fixed dental prostheses, RBFDP) we wanted to investigate whether the abrasion angle alter the surface topography enough to alter the behavior of the bonding agent on the surface. Understanding the effect of the abrasion angle is important at it is not possible, for example, to abrade the inner walls of a single crown at a 90° angle, but more of a 45° angle. In this study airborne-particle-abrasion was performed with 2 bar, 1 bar and 0,5 bar to consider the commonly used range of clinical airborne-particle abrasion devices and inaccuracy of manometers of these instruments.

The material surface properties such as surface free energy play an important role for the bonding of the zirconia. Since it is not possible to directly measure the surface free energy of a solid material, indirect methods are needed. The most common method is to measure the contact angle of different liquids with known parameters (density, surface energy, viscosity, and polarity) on the surface of the solid. (22) Surface energy is always composed of two components, one that relates to the omnipresent dispersive interactions caused by London dispersion forces (e.g., van der Waals forces) between molecules or atoms that are usually symmetric in terms of their electron distribution (non-polar) and one that relates to polar interactions between permanent dipole molecules with nonsymmetrical electron distribution, such as water. (23) In this study, we used a derivation of the Young's equation (OWRK model (24)) to determine the surface energy of the different zirconia surfaces.

1.1 Purpose of the studies

The aim of this study was to determine the surface energy of sandblasted zirconia, and if airborne-particle abrasion with parameters normally used clinically affects the apparent surface energy. Our main research question was whether there is a significant difference between two different angles of airborne-particle abrasion and the use of three different pressures to determine if this has an impact on the physical and chemical surface properties. We also want to compare the 2^{nd} and 3^{rd} generation of zirconia to

determine if these materials could be treated the same way, even though they have very different phase composition and mechanical properties.

2. Materials and Methods

2.1 Zirconia specimens

In this study we utilized two different zirconia types. One soft-machined translucent Y-TZP Prettau Zirconia or ICE Zirconia translucent (Zirkonzahn, Gais South Tyrol, Italy) further referred to as Prettau Posterior. Prettau Posterior is described as a high translucent zirconia with 4-6% yttria (2nd generation). The other zirconia material, Prettau Anterior (Zirkonzahn, Gais South Tyrol, Italy), has been promoted as an ultra-translucent zirconia with a content of maximum 12% yttria (3rd generation). This material is

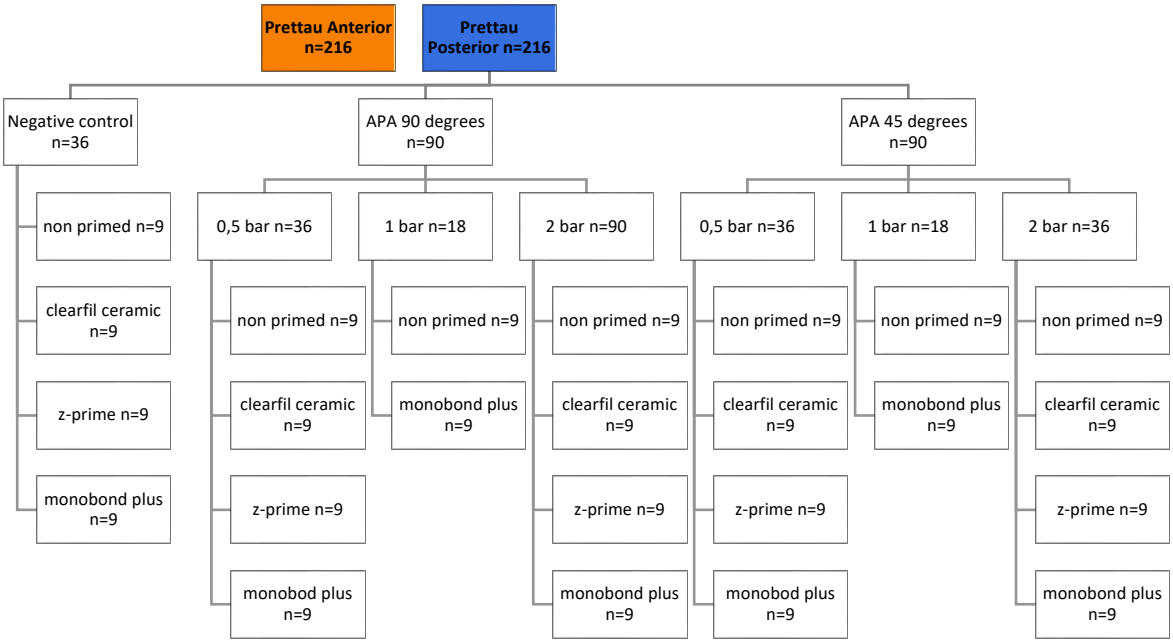

Figure 1: Flow chart of specimens for our zirconia specimens. Prettau Anterior and Prettau Standard with identical disc specimens after APA.

further referred to as Prettau Anterior zirconia. Disc-shaped specimens of both materials were prepared with a thickness of 1,2 mm and a diameter of 13 mm according to ISO 6872 standard for biaxial fracture strength.

2.2 Surface treatment – Specimen preparation

The discs were ground at 500 grit silicon carbide paper to dimensions mentioned and parallelism of the flat surfaces. Excess dust was removed using a clean, soft porcelain brush and compressed air. The specimens were treated equally on both sides, so the available surfaces for testing were double the number of discs. All discs were subsequently sintered in a furnace programmed for the different materials according to the manufacturer (Zirconofen 700, Zirconzahn, Gais, Italy).

The specimens from each of the two zirconia materials were randomly assigned for seven different groups (Figure 1): Two different blasting angles in two subgroups (90° and 45°) and different pressure in three airborne-particle abrasion groups (0,5 bar, 1 bar and 2 bar), and finally one control group for both zirconia materials.

2.2.1 Airborne-particle abrasion (APA)

The abrasive of choice was aluminium oxide (Al_2O_3, Korox-50-BEGO) with a grit size of 50 µm. Airborne particle abrasion was performed with 2 bars, 1 bar and 0.5 bar. The air abrasion nozzle was

mounted on an adjustable holder and the discs were sandblasted for approximately 20 seconds at pressures described above, and the discs oscillated back and forth while air abrasion were performed perpendicular and in an angle of 45° to the surface at 10 mm. The air abrasion technique was standardized through ten test discs, the time for each procedure (angle and pressure) where clocked and were repeatable for the last eight tests. The discs were colored with a marker pen for even airborne-particle abrasion distribution of the whole surface. After surface treatment, all specimens were thoroughly cleaned by steamer and ultrasonically rinsed with ethanol for 10 min, steamed once again and thoroughly air-dried before the surface energy analyses.

2.3 Wettability of zirconia discs

Surface energy of the air-abraded zirconia surfaces was determined using the OWRK-model (24). For this purpose, the contact angle of several liquids with varying surface energies (Table 2) on the sample surface was measured. OCA 20 goniometer (Dataphysics, Germany) was used to measure the contact angle for each test liquid on three non-overlapping areas on three sample discs per group (n = 9). The contour of a 1 µl sessile drop of each test liquid on the sample surface was recorded at room temperature, and the contact angle was determined using SCA20 V.3.7.4 software. Depending on the droplet shape, different fitting parameters were applied to determine the contact angle (CA): ellipse fitting for 30° < CA < 90° tangent fitting for CA < 30° and Young-Laplace algorithm for CA > 90°.

Table 2: Liquids for contact angle measurement with known surface free energy for the polar and the dispersive component.

Surface energy values liquid (mN/m)			
	σ^p	σ^d	σ^{total}
Diiodomethane	2,3	48,5	50,8
Formamide	18,4	39,5	57,9
Glycerol	26,4	37	63,4
Water	51	21,6	72,6

With each alternation between liquids, the syringe of the goniometer was cleaned with 2% sodium dodecyl sulfate (SDS), and bath sonicated in deionized water for 3 minutes. The syringe was then thoroughly rinsed with ethanol and dried with pressured air. All the values were recorded in each group and the mean value was calculated.

Table 3: List of materials used in this study and their main compositions according to the manufacturers. MDP: 10-methacryloxydecyl dihydrogen phosphate, HEMA: 2-hydroxyethyl methacrylate. BPDM: biphenolic dimethacrylate.

System (code)	Main composition	Manufacturer	Lot no.
Monobond Plus Universal primer	*MDP, silane methacrylate, ethanol, sulfide methacrylate*	*Ivoclar Vivadent*	*Y51618*
Clearfil Ceramic Primer Plus	*MDP, silane, ethanol*	*Kuraray Noritake Dental*	*7L0055*
Z-Prime™ Plus Zirconia, Alumina and Metal Primer	*MDP, BPDM, HEMA, ethanol*	*Curion (BISCO Dental)*	*2000002125*
Ivoclean Cleaning paste	*sodium hydroxide, ZrO_2, water, polyethylene glycol, pigments*	*Ivoclar Vivadent*	*X56369*

The surface energy was also determined on the same zirconia surfaces following application of commercially available primers (Table 3).

The primer was applied on the entire disc surface with a micro brush that is for clinical use according to manufacturer's instructions. All primers in Table 3 were tested with deionized water droplets to confirm our assumptions. All samples for all groups were only measured for Monobond, the other two primers were only tested on control and both 2 bar surfaces per zirconia (as the presumably roughest treatment).

The different surfaces were tested nine times per subgroup, per liquid, and the mean of these measurements were used to calculate the interpolation line of the three test liquids.

2.3.1 Cleaning of discs after treated with primer

Because we had a limited number of discs, compared to the number of samples that where necessary to get a significant result, it was necessary to clean the discs thoroughly so there were no rest polymers after the priming process and no organic material left from our different solutions.

We applied Ivoclean solution (Ivoclar Vivadent, Liechtenstein) on the entire surface of the discs for 20 s according to manufacturer's instruction. The discs were then rinsed with deionized water before bath sonication in 2% SDS, deionized water and ethanol for 3 min each. The specimens where then allowed to dry on clean filter paper sheets before they were placed on trays with clean aluminum foil. The trays were then placed in Novascan PSD-UV4 Ozone Cleaner (Novascan Technologies, Inc., USA) for 15 min to remove any remaining organic contaminants and create atomically clean surfaces.

After 48 h storage in fume hood, the discs were packed in paper towels and zip lock bags as previously described.

2.3.2 Surface energy parameters

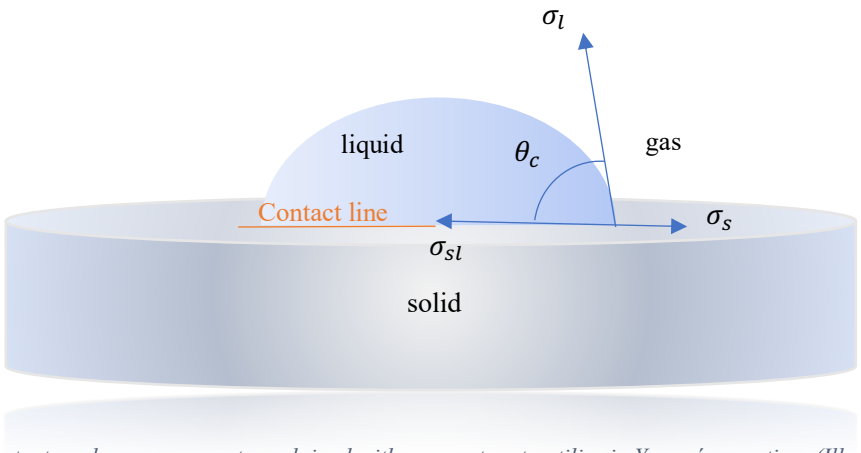

Figure 2: Contact angle measurements explained with parameters to utilize in Young's equation. (Illustration made by author)

Surface free energy must be measured utilizing methods with contact angle measurements. The contact angle method was used to calculate the surface energy parameters utilizing Young's equation:

Equation 1: Young's equation

$$\sigma_s = \sigma_{sl} + \sigma_l \cdot \cos\theta$$

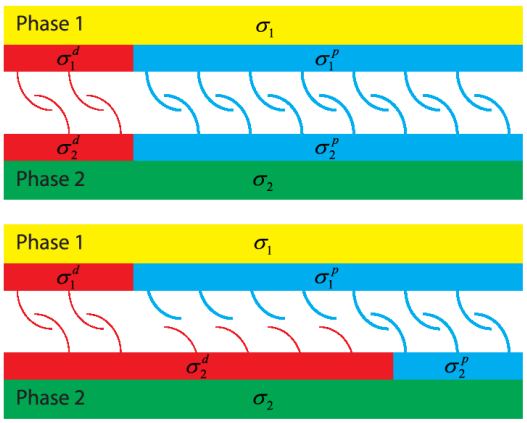

Figure 3: Figure that represents the interactions between two phases with similar (top) or different (bottom) dispersive and polar parts of the surface energy/tension. (26)

where θ is the contact angle and σ_s, σ_{sl}, and σ_l are the surface tensions of the solid, solid–liquid, and liquid surfaces, respectively (Figure 2). Young's equation gives us the relationship between the contact angle and the solid-liquid interfacial energy. (25)

Hence, by measuring the contact angles of four liquids with known surface energy parameters on solid surfaces, the solid surface free energy, and its components can be calculated using linear regression with the least square method. In addition, the total surface energy σ_s of the materials is derived by the equation.

The total surface free energy of a surface can be explained as the cause of the interaction between polar and dispersive components. (23) This is shown in Figure 3. The interaction between the polar and dispersive is described with the equation:

Equation 2: Surface free energy

$$\sigma_i = \sigma_i^d + \sigma_i^p$$

where the surface free energy or surface tension σ_i of component i , in this case the surface of the zirconia disc, is additively made up of dispersive σ_i^d and polar parts σ_i^p. (26)

The surface free energy of the liquids is known (see Table 3), hence can be used to calculate the effect of the polar and dispersive component combined and as a result find the surface free energy of a solid. We did this using the OWRK model of *Owens, Wendt, Rabel* and *Kaelble*, in the form of a linear equation of the type y = mx + c. (27)

Equation 3: OWRK model

$$\underbrace{\frac{\sigma_L\,(1+\cos\theta)}{2\sqrt{\sigma_L^d}}}_{y} = \underbrace{\sqrt{\sigma_S^p}}_{m} \cdot \underbrace{\sqrt{\sigma_L^p / \sigma_L^d}}_{x} + \underbrace{\sqrt{\sigma_S^d}}_{c}$$

Contact angles were converted from degrees to radians. After plotting in our known parameters for polar and dispersive components combined with known surface free energy of the liquids, we got a plot where:

$\underbrace{\frac{\sigma_L(1+\cos\theta)}{2\sqrt{\sigma_L^d}}}_{y}$ is the y-axis and $\underbrace{\sqrt{\sigma_L^p/\sigma_L^d}}_{x}$ is the x-axis.

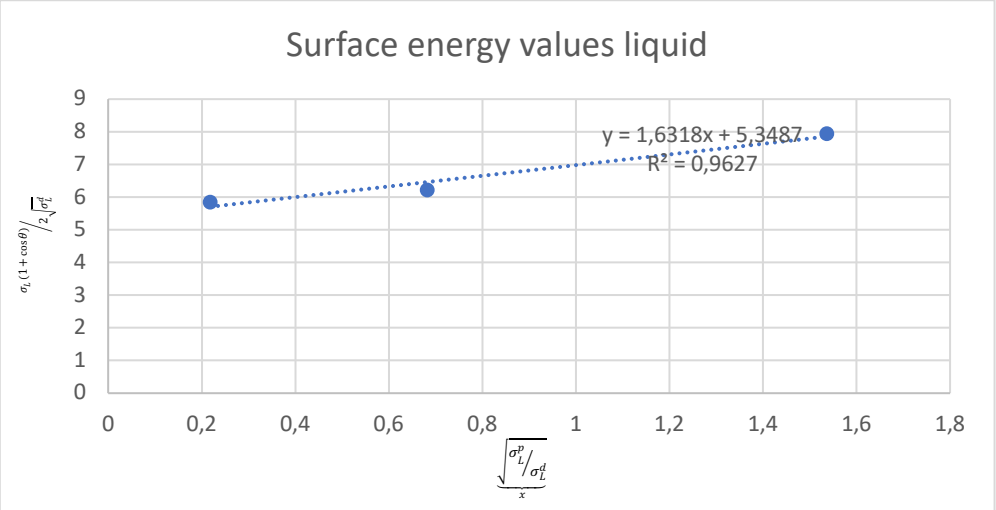

Figure 4: OWRK method using graph showing a linear regression of surface free energy for different liquids.

By looking at the parameters of the line we were given a slope that became our m value, $\underbrace{\sqrt{\sigma_S^p}}_{m}$, and a crossing point that became our c value, $\underbrace{\sqrt{\sigma_S^d}}_{c}$, in the OWRK-model. By summing up the dispersive and polar parts together we got the total surface free energy $\sigma_i^d + \sigma_i^p = \sigma_i$.

2.4 Profilometry: Roughness of zirconia discs

The roughness of the zirconia discs was evaluated by profilometry measurements by means of an 3D optical profiler (S Neox optical profiler, Sensofar, Barcelona, Spain) controlled with the SensoSCAN 6.3 software, also from Sensofar. Samples were imaged with an EPI 150× (NA0.95) objective using the brightfield mode with area field of view of 113 × 94 µm^2. All images were flattened by subtraction, reconstructed, and numerically processed to 3D topographical parameters using SensoMap Standard 7.3 (Sensofar, Digital Surf's Mountains Technology®, Spain).

All profilometry results were obtained from the measurements performed at three randomly distributed non-overlapping spots on three different samples per surface treatment (n=9) The calculated surface roughness values (Sa) are presented as the mean ± SD.

2.5 Scanning electron microscopy (SEM)

A scanning electron microscope equipped with energy-dispersive x-ray spectroscopy (EDX) was used for chemical surface characterization (TM3030, Hitachi, Japan). The sample discs (n = 3) were mounted on aluminium stubs using conductive double-sided carbon tape and imaged using backscattered electrons at 15 kV acceleration voltage. Characteristic x-rays emitted from the sample surface were detected using Bruker XFlash EDX systems and the elemental composition of the sample surface was analysed with Quantax 70 software (Bruker, USA).

Susanna Patiño Walbækken
Arne Sebastian Rossow

2.6 Statistical analysis

Results were analyzed by one-way analysis of variance (ANOVA) to compare the surface treatments for each specimen group. All statistical analyses were performed using the SigmaPlot version 14.0 software system (Systat Software, San Jose, CA). Pairwise multiple comparisons were performed using the Holm-Sidak method. Values are presented as mean ± standard deviation and statistical significance was considered at $p < 0,05$.

3. Results

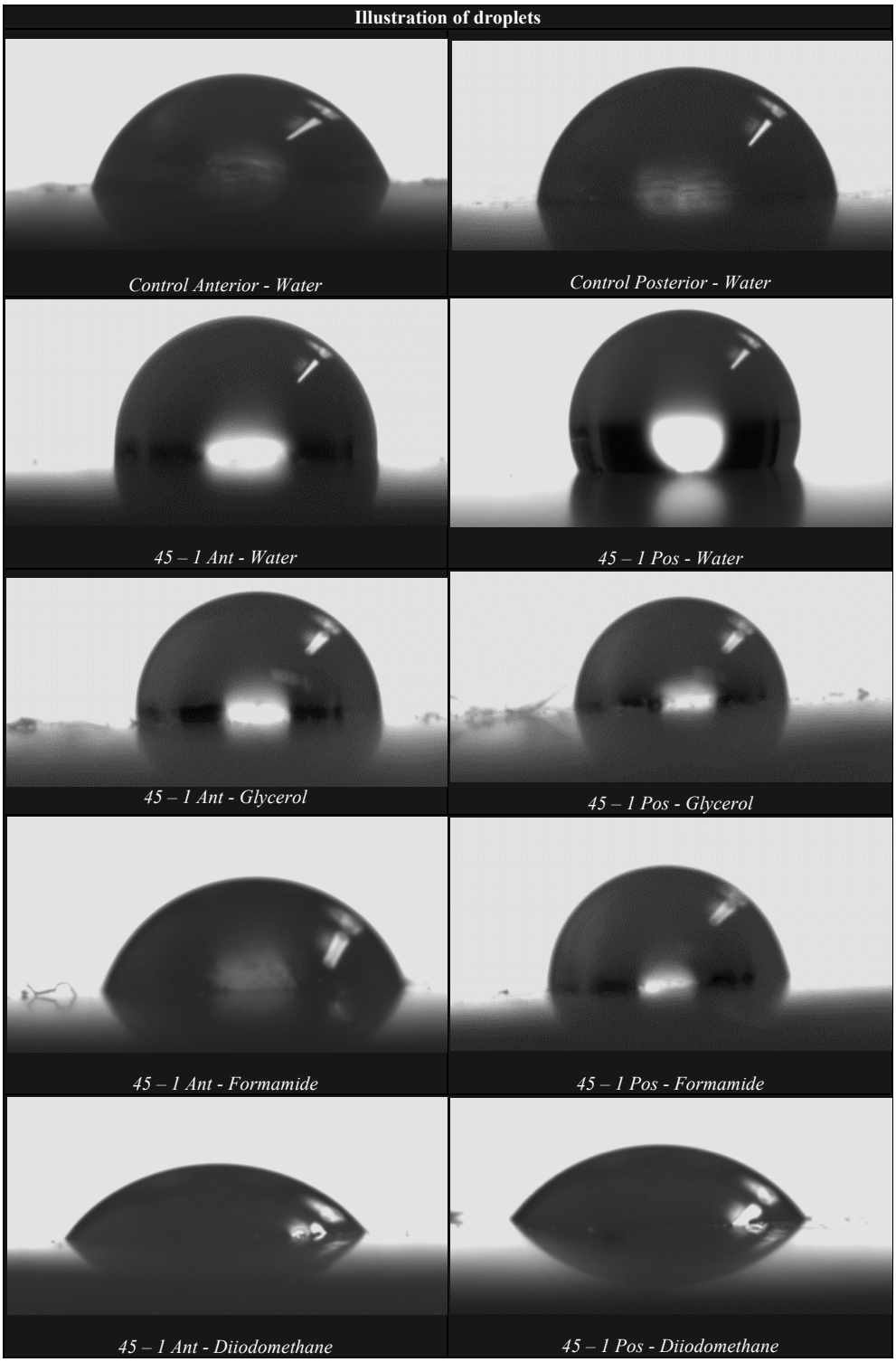

Figure 5: Pictures of results taken during droplet measuring with The OCA 20 by Dataphysics where the contact angle was determined using SCA20 V.3.7.4 software. Images in order of decreasing surface energy of the test liquid.

Figure 5 shows the observed droplet shape of the different test liquids on zirconia coins with 1 bar, 45° airborne-particle abrasion with the four different liquids used. You can see a difference in how the different liquids behaved on the surface, with the contact angle decreasing as the total surface energy of the test liquid decreased. The water droplet has the highest contact angle, while the diiodomethane has the lowest contact angle. Water is the most polar test liquid, while diiodomethane is the most dispersive, suggesting that the sandblasted zirconia surface is more dispersive than polar. Glycerol contact angles were measured, but not included in the calculation for surface free energy, because they were consistently out of the linear fit. Comparing the water droplet on the control and 45-1 bar, the contact angle is higher on the sandblasted surface than on the control surface. In between the posterior and anterior zirconia, there are very small differences, and in general, they seem to behave the same way.

3.1 Roughness of zirconia discs

The roughness is presented as the arithmetical mean surface height deviation (Sa), and it is obtained from the mean value of three measurements taken at random non-overlapping regions on three independent test samples for each group.

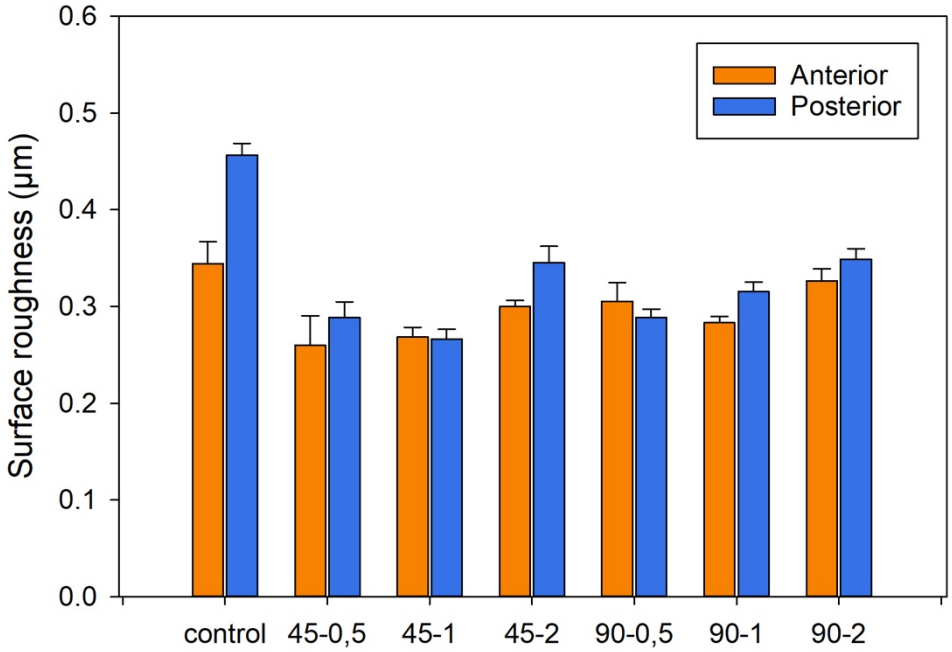

Figure 6: Visual presentation of the surface roughness on the different specimen groups with standard deviation.

Figure 6 shows the results obtained with the profilometer and we can only observe small differences in the roughness on the disc itself and in between the discs in the same group. After statistical analysis we determined that the Posterior sample with APA 45° 2 bar was significantly different than the 1 bar sample in the same APA group, with increased surface roughness. The differences in the mean values among these treatment groups are greater than would be expected by chance. The APA 90° 2 bar sample was only significantly different to the 0,5 bar specimen, but not the 1 bar specimen. The statistically significant increase in surface roughness values for the 2 bar samples supports the overall tendency towards higher roughness values with increasing APA pressure observed in Figure 6.

The result of the equal variance test indicates the likelihood that the two groups, anterior and posterior with APA 45° with both 0,5 and 1 bar in pressure and APA 90° with both 0,5 and 2 bar pressure, are sampled from populations with equal variances, but does not guarantee the equality or inequality of the two variances. The difference in the mean value is not great enough to reject the possibility that it is due to random sample sampling. The difference in the mean values of the two groups posterior and anterior,

with APA 90° with 1 bar pressure and APA 45° and 2 bar pressure, is greater than would be expected by chance; there is a statistically significant difference between the input groups.

In Figure 16 and 17, machining pattern can be seen in the control groups, when measuring the surface roughness. Machining pattern can be seen clearly on 45 – 0,5 and this completely disappears on the other APA treated surfaces. We still see the distinguishable grooves, much more than on the other. This is clearer on the anterior discs.

3.2 Surface free energy of zirconia discs

Table 4 shows small differences in surface energy between the anterior and the posterior zirconias when sandblasted. On the other hand, there is a clear difference between the control group and the treated zirconias. Anterior zirconia has a much higher polar component compared to posterior zirconia, raising the total surface energy on the anterior zirconia to 58,78 mN/m, while the total surface energy was only 29,75 mN/m on the posterior zirconia. The surface energy on the anterior zirconia seems to decrease to the same level as the posterior zirconia when the airborne-particle abrasion pressure increases.

Table 4: Surface energy measurements after calculating the polar and dispersive component in each specimen group. Comparison between non primed and Monobond (primed) surface. Surface energy is presented in mN/m.

Variables			*Non-Primed*			*Monobond (primed)*		
Material	**Angle (Degrees)**	**Pressure (bar)**	**Polar**	**Dispersive**	**Surface energy**	**Polar**	**Dispersive**	**Surface energy**
Anterior	Control		30,48	28,30	58,78	28,57	33,72	62,29
	45˚	0,5 bar	0,64	43,00	43,64	1,13	50,92	52,05
		1 bar	0,13	29,29	29,42	96,43	20,08	116,51
		2 bar	0,55	28,56	29,10	124,86	16,59	141,45
	90˚	0,5 bar	0,58	29,37	29,96	125,60	16,63	142,22
		1 bar	9,69	21,44	31,12	110,86	18,69	129,55
		2 bar	0,14	32,18	32,32	124,17	16,79	140,96
Posterior	Control		6,91	22,83	29,75	34,64	33,83	68,48
	45˚	0,5 bar	0,15	29,95	30,10	3,10	51,16	54,26
		1 bar	1,18	21,73	22,92	96,94	20,83	117,77
		2 bar	0,95	24,01	24,95	82,47	23,03	105,49
	90˚	0,5 bar	0,13	26,75	26,87	108,68	19,29	127,97
		1 bar	2,49	23,87	26,35	125,60	17,32	142,92
		2 bar	0,26	24,80	25,06	121,75	17,89	139,64

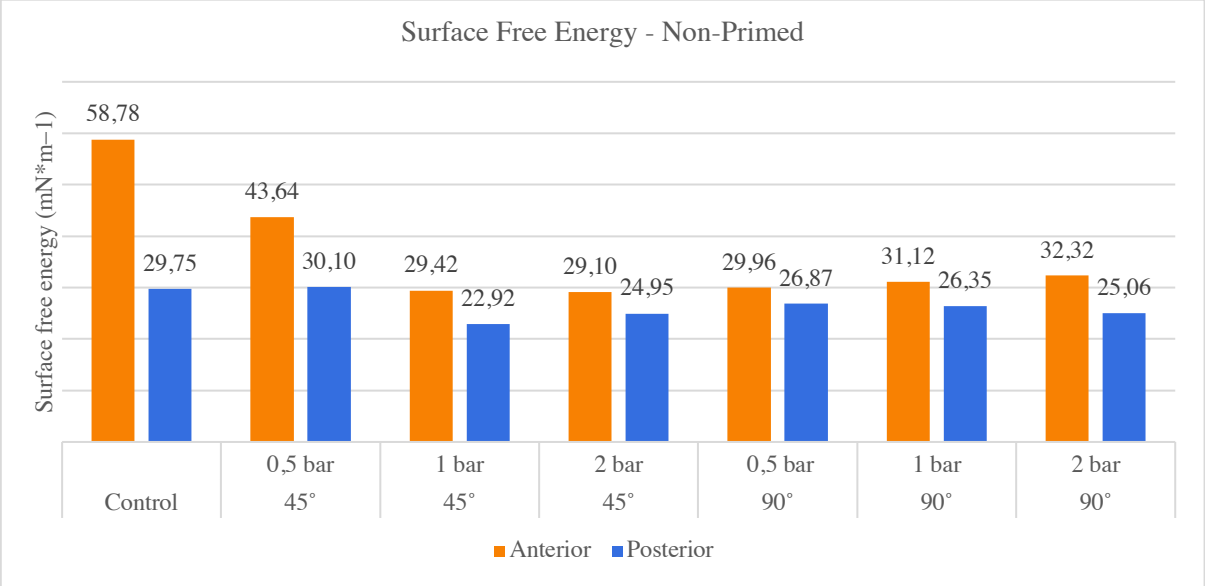

Figure 7: Surface free energy measurements after calculating the polar and dispersive component in each specimen group. Non-primed surface.

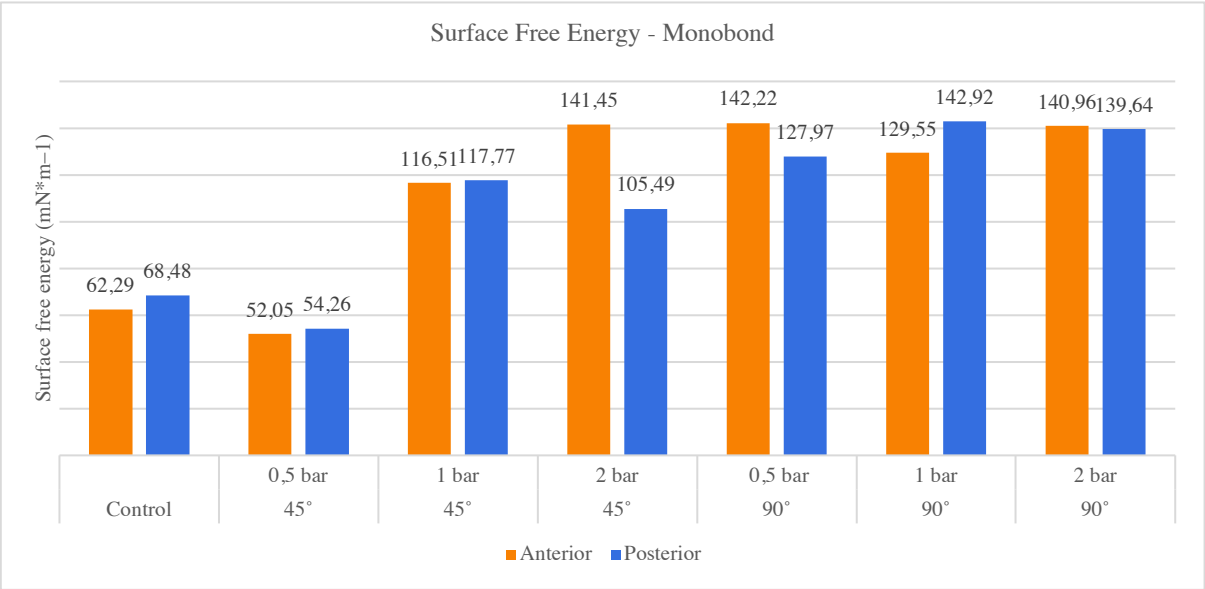

Figure 8: Surface free energy measurements after calculating the polar and dispersive component in each specimen group. Surface primed with Monobond.

On primed surfaces, we see very small to no differences between the posterior and anterior zirconia. There are almost no differences between the surfaces treated with APA 90°. Priming had limited effect on the surface energy of APA 45° 0,5 samples on either type of ZrO_2. On all other surfaces the polar component of the surface energy was significantly increased. This resulted in an increased the total surface energy of the sample.

Susanna Patiño Walbækken
Arne Sebastian Rossow

Table 5: Influence of surface treatment on the surface free energy of zirconia ceramics determined by the measurement of contact angles with 3 different liquids

Variables			*Z-PRIMER*			*CLEARFIL CERAMIC*			*MONOBOND*		
Material	**Angle**	**Bar**	**Polar**	**Dispersive**	**Surface energy**	**Polar**	**Dispersive**	**Surface energy**	**Polar**	**Dispersive**	**Surface energy**
	Control		28,99	29,49	58,48	28,96	5,81	34,77	28,57	33,72	62,29
Anterior	45˚	2	103,00	20,52	123,52	68,13	27,20	95,32	124,86	16,59	141,45
	90˚	2	124,17	16,79	140,96	82,00	25,00	107,00	124,17	16,79	140,96
	Control		129,37	16,96	146,32	40,65	34,14	74,79	34,64	33,83	68,48
Posterior	45˚	2	113,96	19,11	133,06	93,38	23,27	116,65	82,47	23,03	105,49
	90˚	2	126,32	17,89	144,21	81,74	24,93	106,67	121,75	17,89	139,64

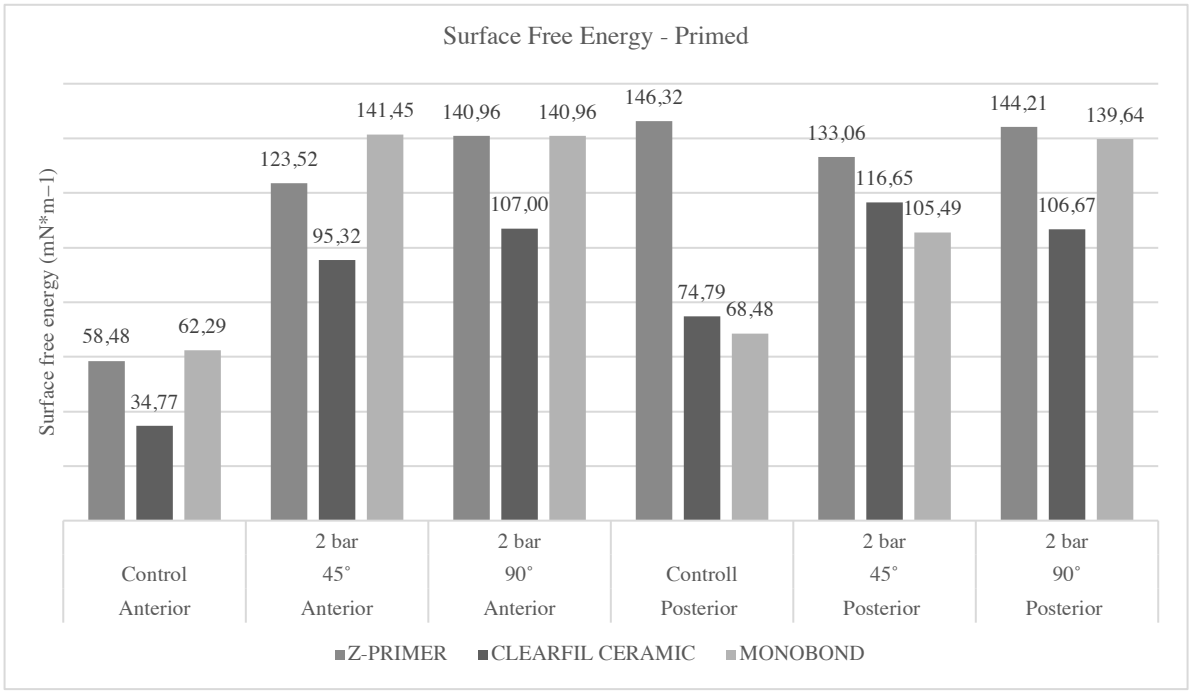

Figure 9: Visual representation of surface treatment on the surface free energy of zirconia ceramics determined by the measurement of contact angles with 3 different liquids.

Comparing the primers with each other (Figure 9) shows that the primers behave quite the same. Clearfil Ceramic has generally a bit lower surface energy than the other primers. Z-prime is almost identical to the Monobond on every aspect, except from control posterior.

After being through the UV/ozone cleaner the discs changed to a darker color (Figure 10), from white to beige immediately after UV/ozone cleaning but returned to their usual color after exposure to ambient

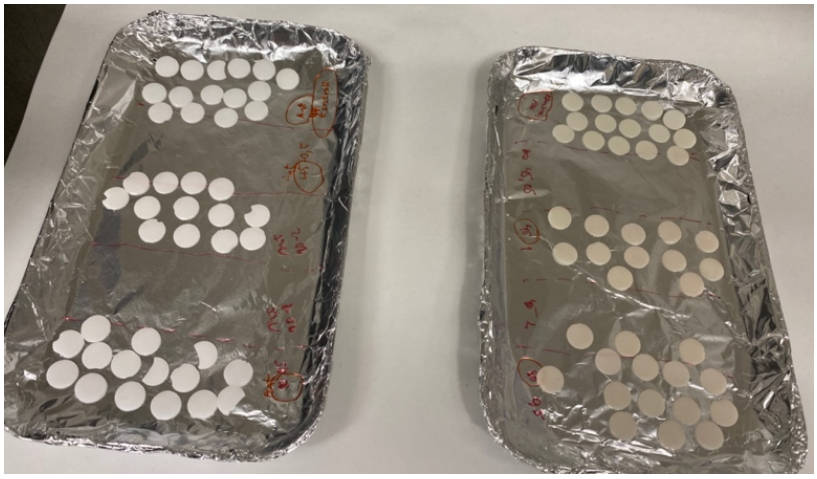

Figure 10: Anterior discs on the left and posterior on the right after UV/Ozone cleaning.

air. For anterior ZrO_2 samples, this color changed happened within a matter of minutes but for the posterior material it took several hours. The original color did not return until overnight exposure to ambient air. Because of this we were unsure if the surface had been changed and we made further measurements on these discs right after going through the UV/ozone cleaner.

The discs where tested right after UV/ozone cleaner, without letting them rest over the night. The angles where significantly lower than previous measurements where we left the specimens overnight, as you can see in Figure 11. We also observe that we do not have the same effect when only cleaning with SDS and ethanol.

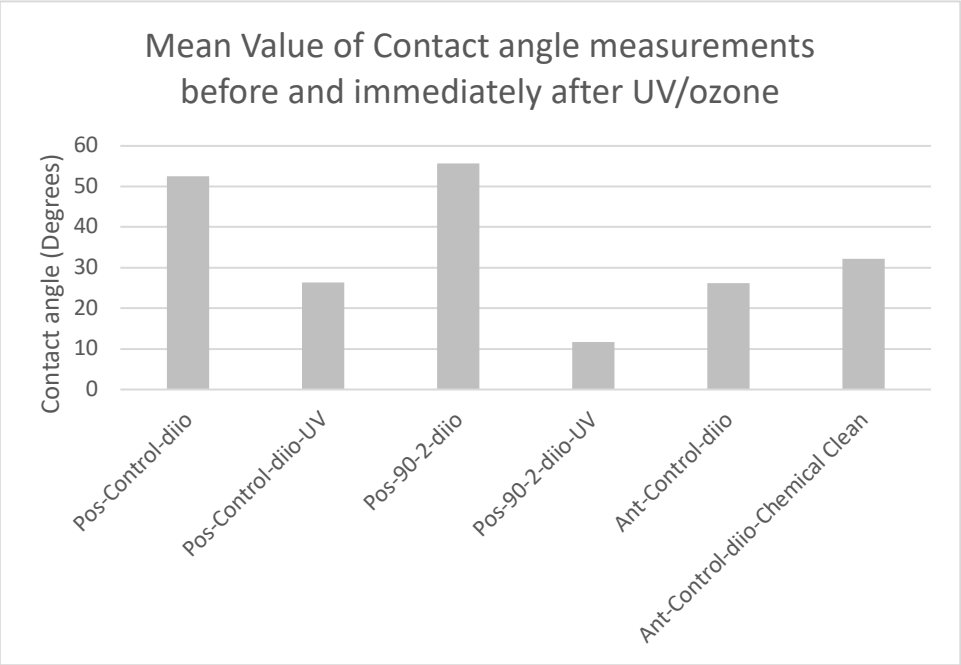

Figure 11: Comparison of contact angles before and after UV/Ozone cleaning

3.3 Surface contamination after airborne-particle abrasion with aluminum oxide

Table 6: Surface contamination after APA treatment (wt.%)

Anterior	*Oxygen*	*Zirconium*	*Carbon*	*Yttrium*	*Aluminium*	Sum
Ant-45-0,5	23,64	56,47	9,28	7,38	1,49	98,26
Ant-45-1	23,46	59,33	3,99	7,50	2,29	96,57
Ant-45-2	25,52	62,05	4,25	8,17	3,17	103,16
Ant-90-0,5	23,07	58,93	4,22	7,51	2,22	95,95
Ant-90-1	23,22	55,61	3,84	7,08	2,06	91,82
Ant-90-2	23,15	55,09	6,59	6,39	2,97	94,19
Ant-con	21,05	66,02	4,44	8,36	0,09	99,96
Posterior						
Pos-45-0,5	22,27	61,13	5,68	4,14	1,85	95,07
Pos-45-1	22,91	67,21	4,86	4,85	1,41	101,24
Pos-45-2	25,28	61,20	5,75	4,81	2,92	99,96
Pos-90-0,5	22,56	60,63	4,61	4,20	1,62	93,63
Pos-90-1	25,88	64,04	5,23	4,71	2,42	102,27
Pos-90-2	24,71	42,97	20,55	4,26	3,07	95,56
Pos-con	21,52	64,71	5,81	4,48	0,11	96,62

Table 6 shows that the airborne-particle abrasion pressure affected the alumina content on the surface. This table shows higher alumina content when airborne-particle abrasion was performed with 2 bar compared to 0,5 and 1 bar. Table 6 shows that the zirconia surfaces also became contaminated by carbon. Around 5 wt.% of the surface is carbon atoms.

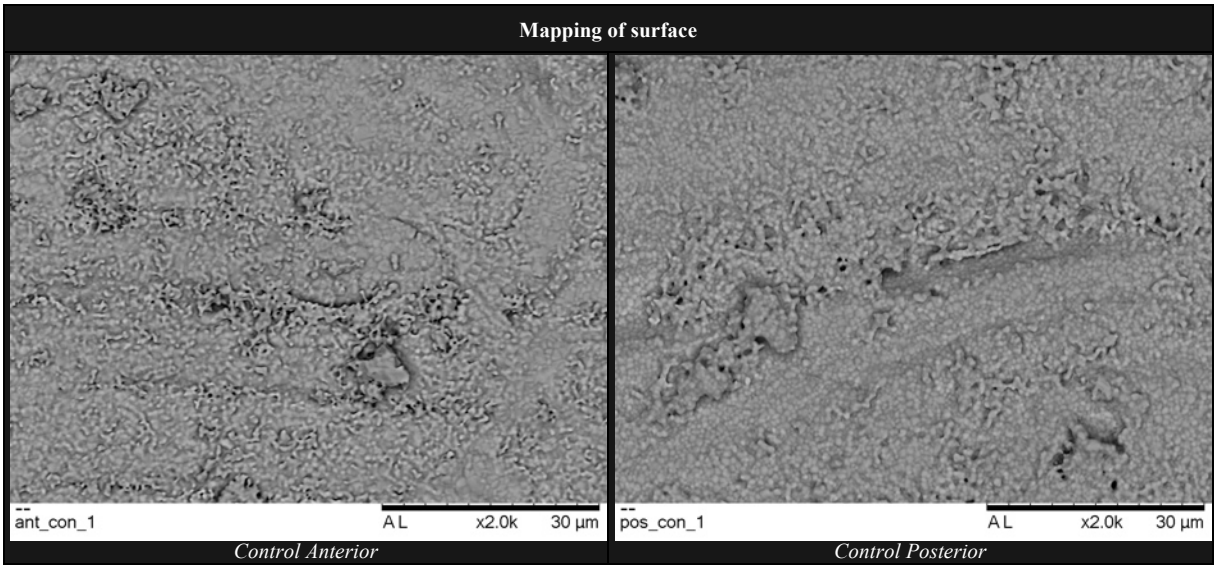

Figure 12: Mapping of control discs. Comparison between anterior and posterior

The SEM images of the control surfaces for anterior and posterior zirconia are presented in Figure 12. Although microroughness can clearly be observed on these images, the anisotropic microgrooves seen on the control surfaces in the 3D images obtain by profilometry were not visible in the SEM images. However, when the BSE imaging mode was switched to topography mode in the SEM by switching of one of the detector panel, the machined pattern was revealed on the sample surface (Figure 13, left panel)

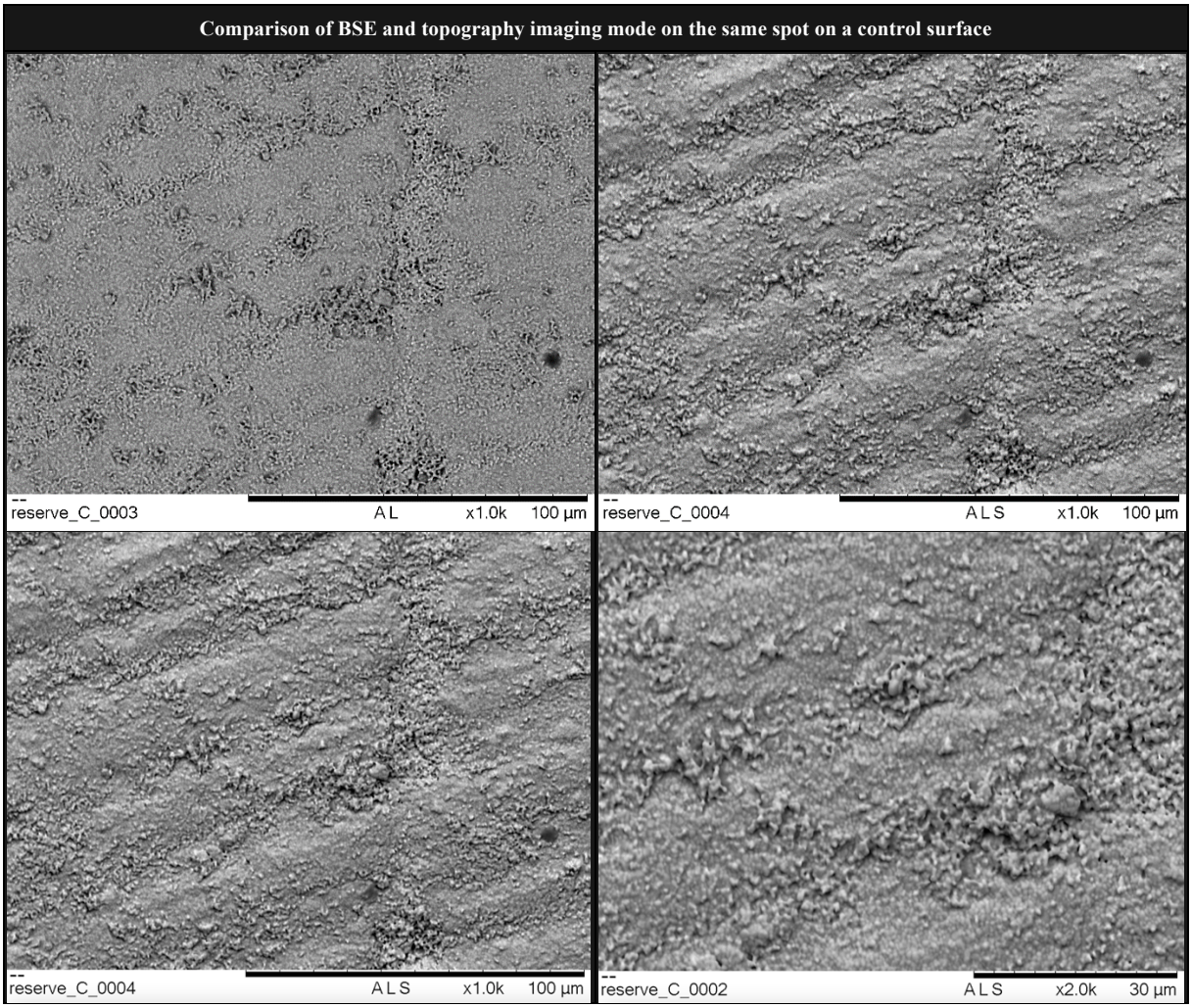

Figure 13: Mapping of surface on reserve discs. Discs were not chemically cleaned or treated with APA. No prior testing on these discs.

On the mapping images (Figure 14), it is possible to see where the different elements are on the surface. The first images show zirconia, yttria and oxygen in different shades of blue. These elements are widely and evenly spread across the whole surface, while the aluminium, highlighted in orange, is more spread around the surface in clusters, suggesting that these are aluminium particles originating from the airborne-particle abrasion process. When comparing the aluminium (Al) map with the backscattered electron (BSE) micrograph in Figure 14, the aluminium signal detected with EDX directly corresponds to the location of the black spots observed on the BSE image. While such aluminium particles were detected on all APA-treated surfaces (Figure 14), there is almost none of these black spots on the control surfaces (Figure 12 and Figure 13), which compliments the low aluminium content for the control groups in Table 6.

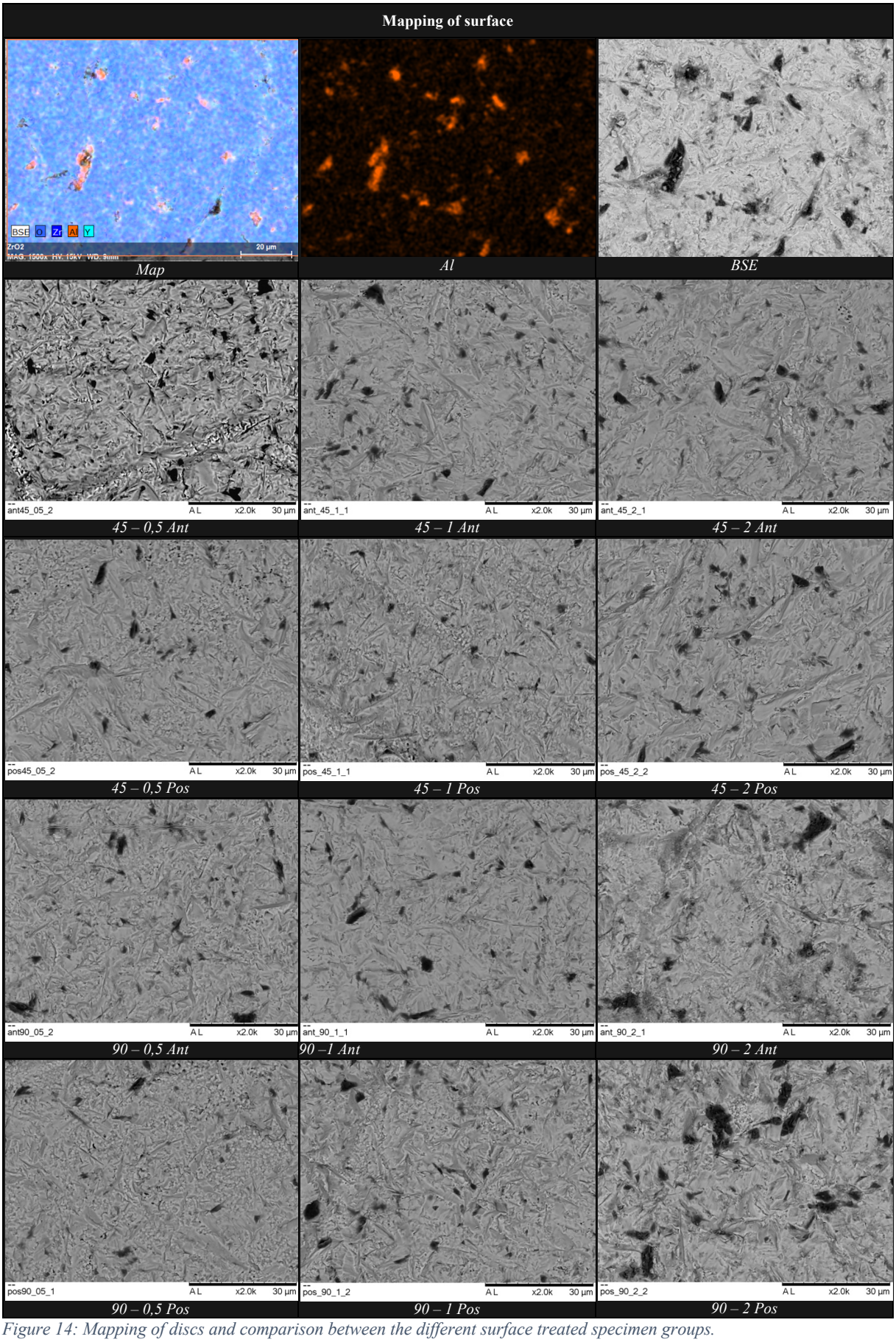

Figure 14: Mapping of discs and comparison between the different surface treated specimen groups.

After statistical analysis, our results showed no significant difference between most groups. The differences in the mean values among the treatment groups APA 45° between 2 bar and 0,5 bar in the anterior group, are greater than would be expected by chance. In the group with posterior discs there was a difference with 2 bar pressure between the APA 90° and APA 45°. Also, in the APA 45° group between 2 bar and 1 bar.

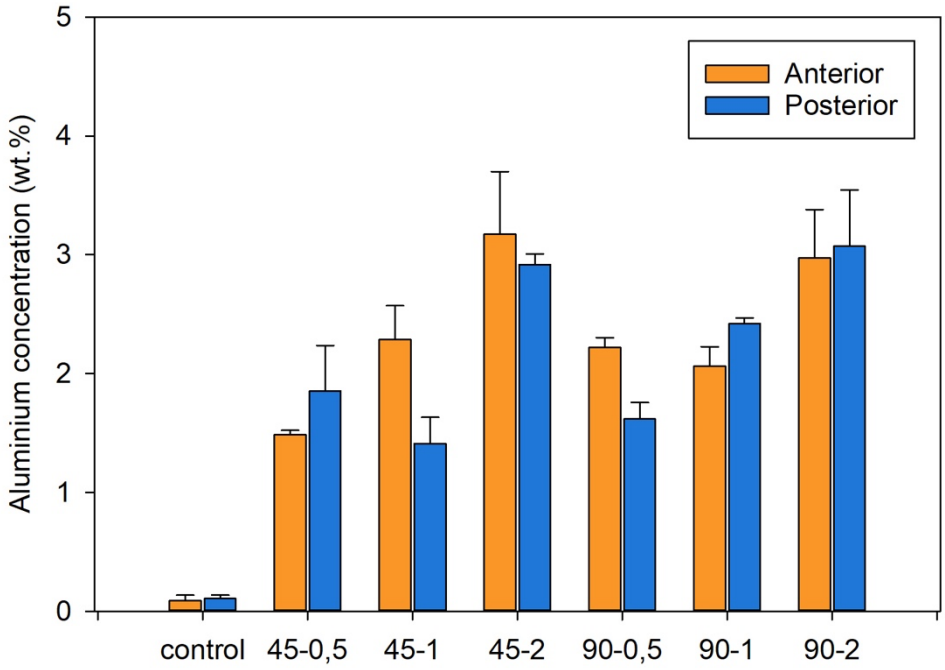

Figure 15: Illustration of aluminium concentration on the different zirconia groups with standard deviation.

3.4 Profilometry imaging

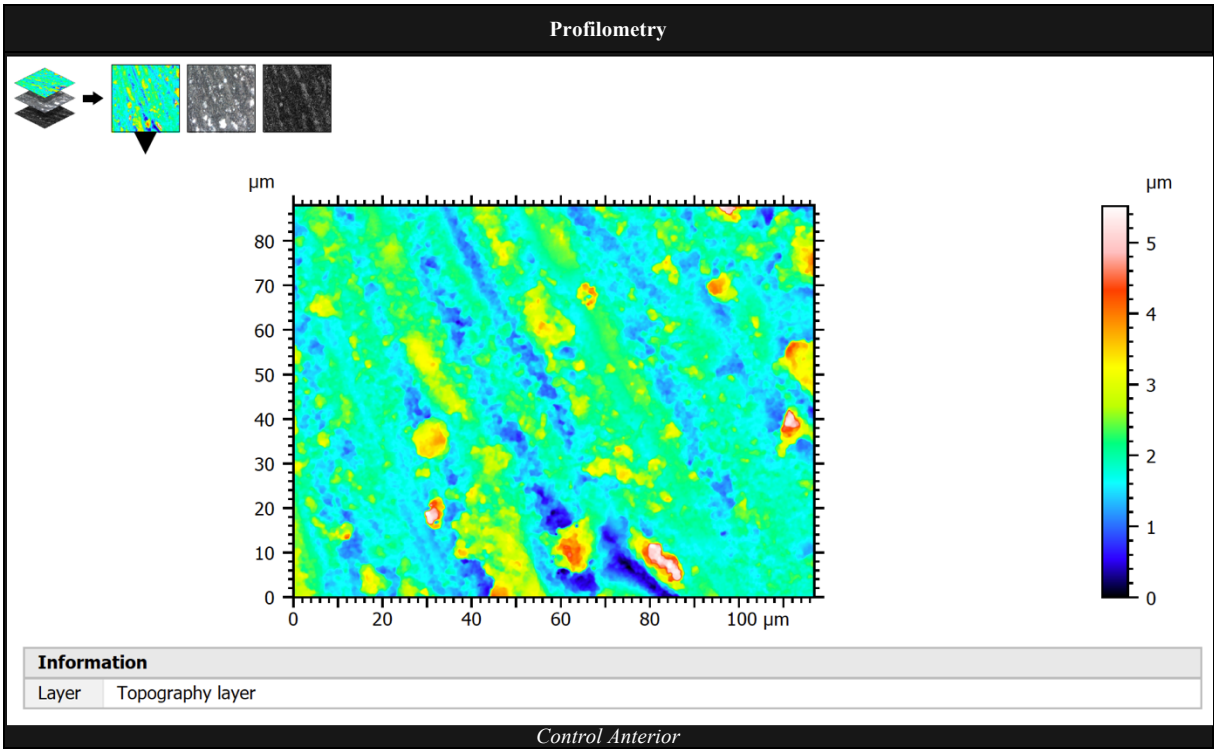

Figure 16: Profilometry. Final topography layer of control anterior disc specimen.

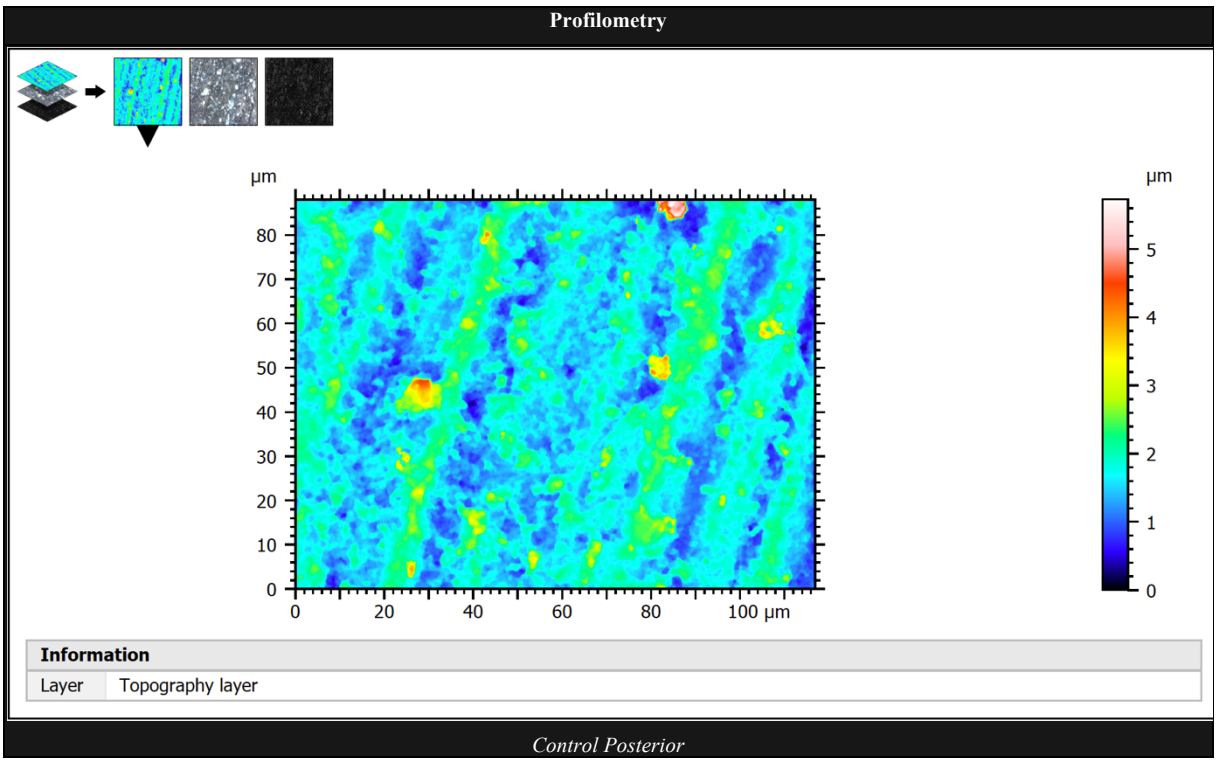

Figure 17: Profilometry. Final topography layer of control posterior disc specimen

Profilometry	
Anterior	**Posterior**
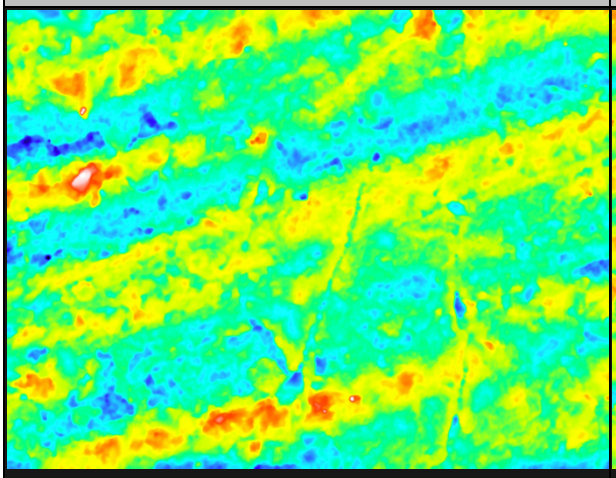	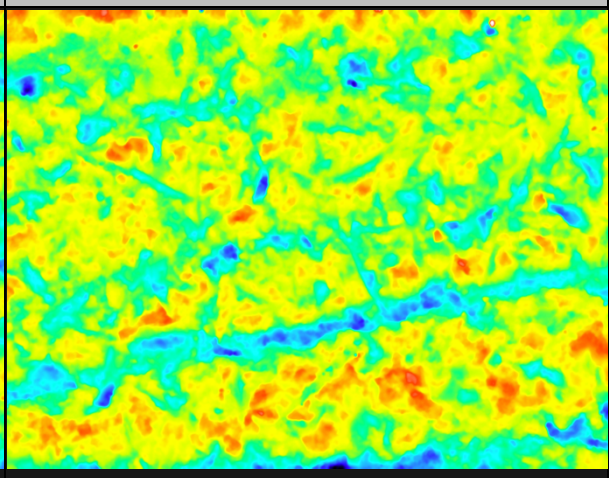
45 – 0,5 Ant	*45 – 0,5 Pos*
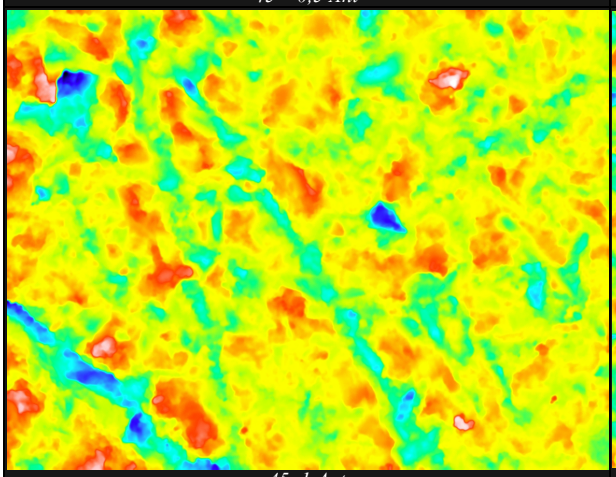	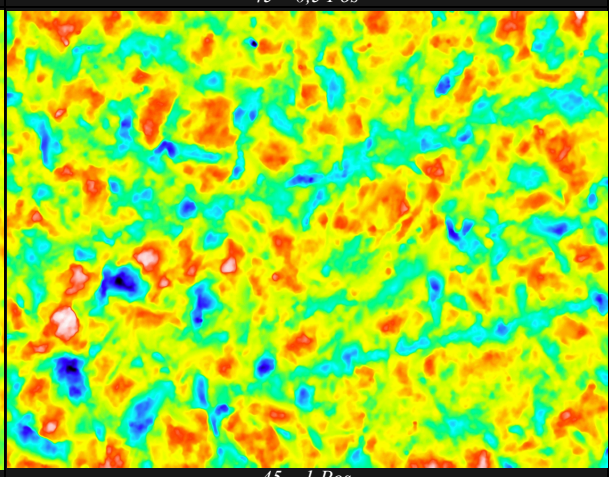
45–1 Ant	*45 – 1 Pos*
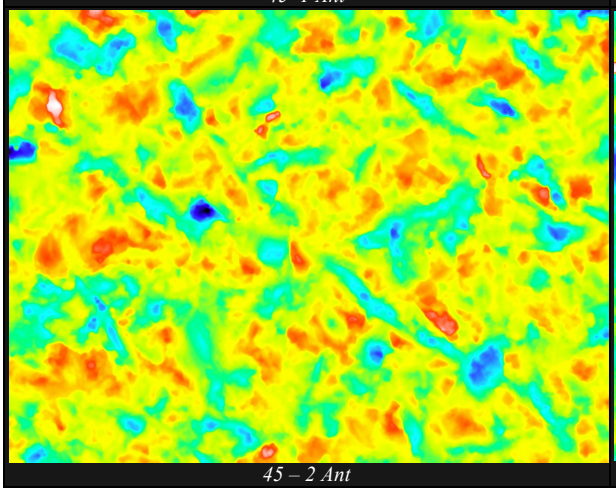	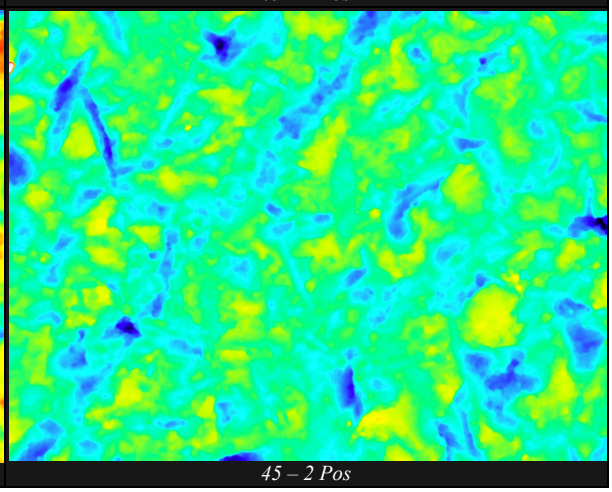
45 – 2 Ant	*45 – 2 Pos*

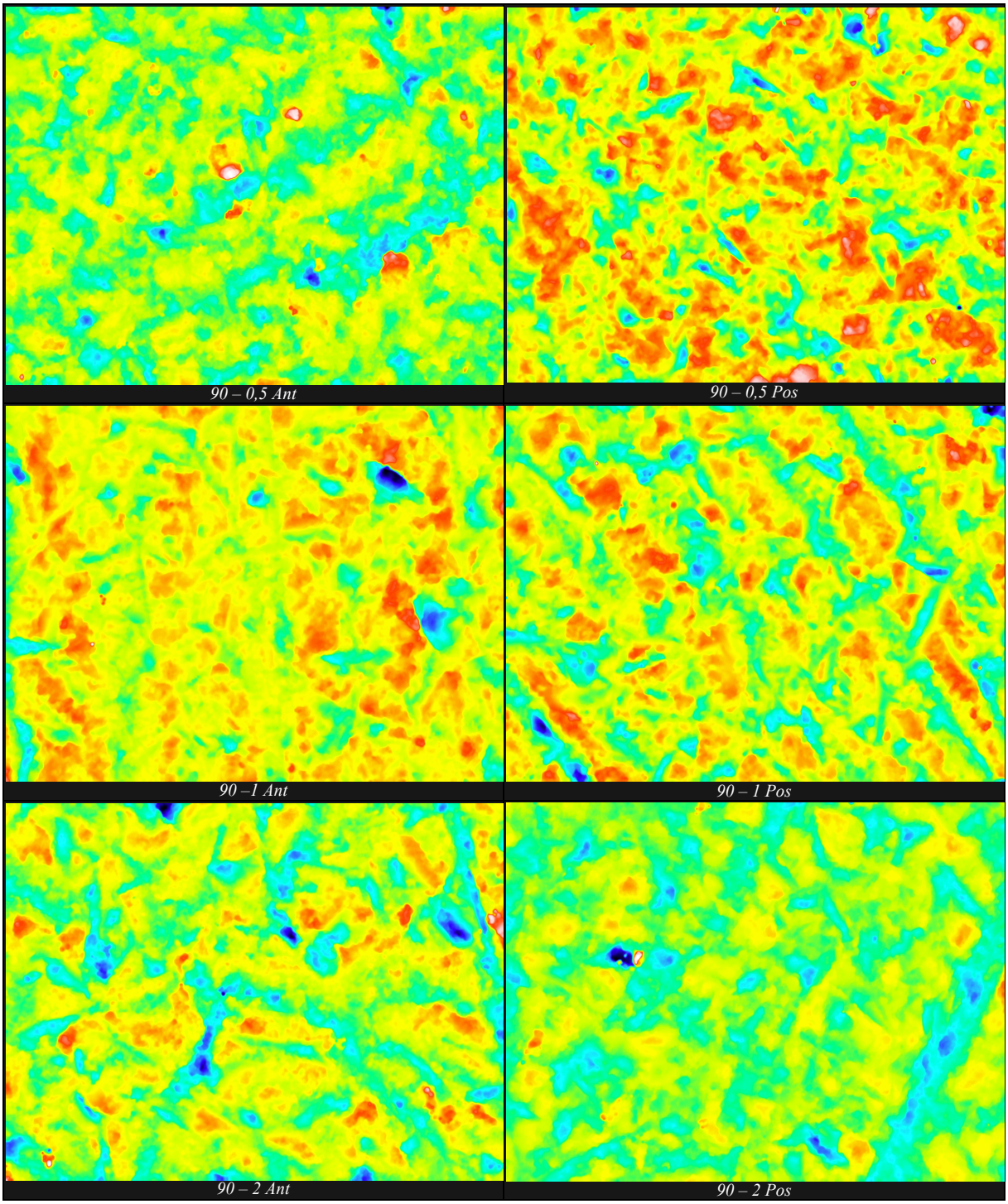

Figure 18: Profilometry. Final topography layer and comparison of all specimen groups after APA.

Figure 18 shows grooves from the machining on all the specimens treated with a pressure of 0,5 bar. The grooves are less visible on the specimens treated at 1 bar and not visible at all on the specimens treated at 2 bar pressure. This difference between the surface texture of samples treated with 0,5 bar and 2 bar pressure becomes even more obvious in the 3D presentation of the surface topography shown in Figure 19. The control specimens and 0,5 bar treated specimens have significant grooves on the surface, but the specimen treated at 2 bar has no signs of machining pattern.

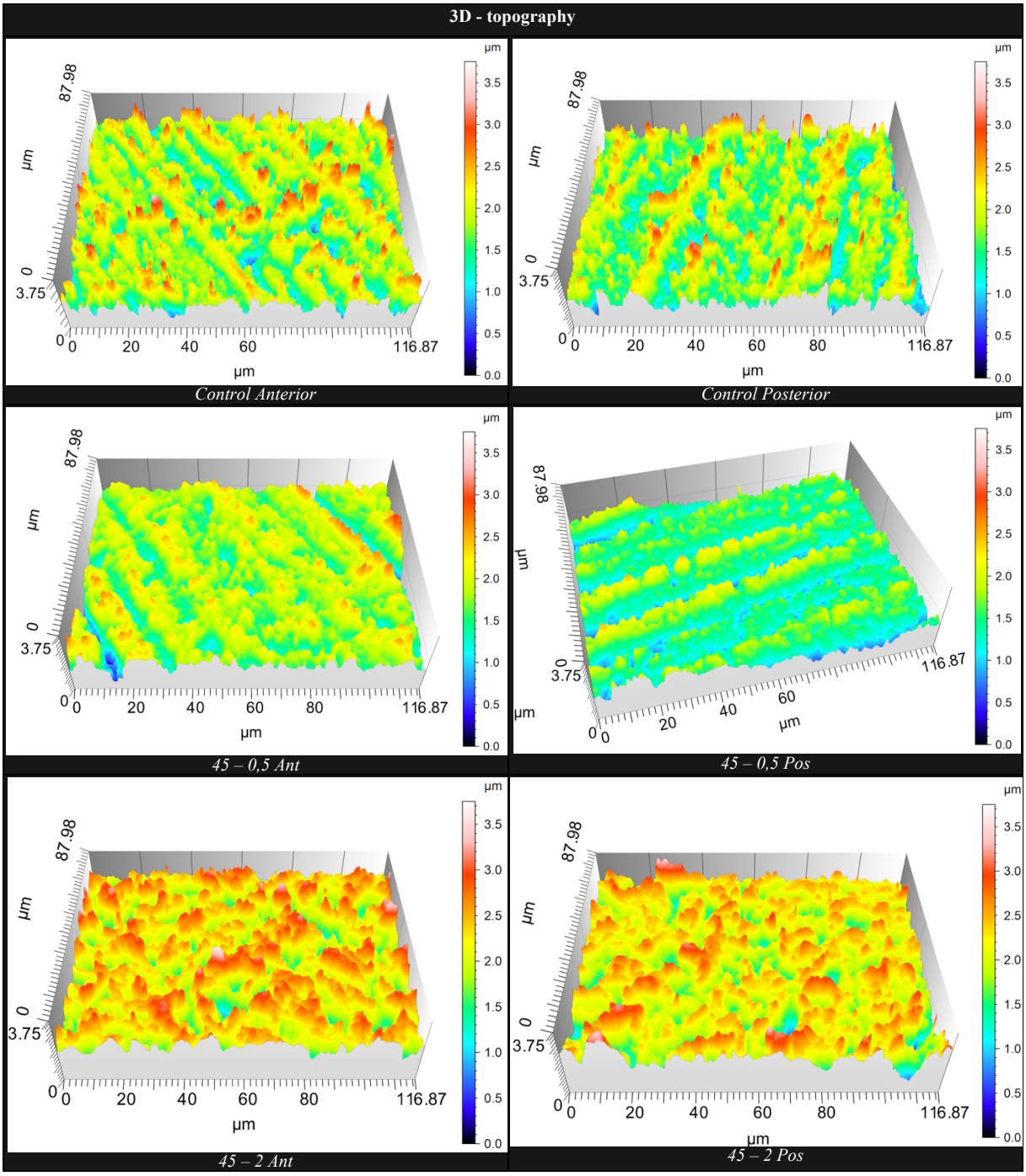

Figure 19: 3D topography comparison of different specimen groups after APA.

4. Discussion

4.1 Color change after UV/ozone cleaner

The observed color change is likely to be caused by change in oxidation state of the superficial Zr ions due to reduction of Zr and formation of oxygen vacancies on the zirconia surface by chemical oxidation during the UV/ozone cleaning procedure. A weak reduction of yttrium-stabilized zirconia to lower surface oxidation states (ZrO_{2-x}) has been shown to alter the color from white to yellow or black, depending on the amount of reduction and oxygen vacancies that form. (28) (29) Since ZrO_2 is the most stable oxidation state for this material, this altered surface oxidation (ZrO_{2-x}) was only temporary, and both anterior and posterior zirconia returned to their original oxidation state over time. Based on the

deeper brownish color and longer time it took for the posterior surface to "recover" to its normal state, we can assume that more reduction occurred on posterior than anterior zirconia surface (29).

Due to the difference in the oxidation state of the metal cations in Y_2O_3 and ZrO_2, addition of yttrium oxide increases the number of oxygen vacancies in yttrium-stabilized zirconia. In the metastable tetragonal phase, these vacant oxygen lattice positions or oxygen diffusion may be more accessible to changes than in the cubic phase. The fact the low temperature phase transformation (aging) in the presence of water and elevated temperatures only happens in 3Y-YZP and not in >5Y-YZP (30) may indicate that oxygen vacancies are more available for oxygen diffusion from the external environment to interact with in the metastable tetragonal phase than in the cubic phase of ZrO_2. We also noticed that after treatment with UV/ozone the contact angle decreased compared to samples without the exposure to UV/ozone. The one we tested by applying a drop of water, before going through the cleaner, had a higher contact angle than the one we tested after we exposed the disc to UV/Ozone. This also stabilized over time as hydrocarbons from the ambient environment adsorbed on to the surface of the cleaned samples.

4.2 Aluminum oxide and surface contamination after APA

The results in Table 6 show a higher contamination of aluminium when airborne-particle abrasion is done with 2 bar pressure. As expected, the alumina particles penetrate the surface on a bigger scale when more pressure is applied. The results between 0,5 bar and 1 bar are somewhat more surprising. We would think that the contamination of aluminium is higher at 1 bar, but our results show no substantial difference. 1 bar is the standard pressure used in a clinical setting, and these results reinforce the assumption that it most probably is the optimal pressure. At 2 bar, the aluminium contamination increases notably. This will probably affect the bonding strength to the cement as well because the alumina will be an extra interface on the surface and neither bond to the cement nor the zirconia.

In addition, our results show no substantial difference between the two angles of APA. We assumed that there would be a higher contamination of aluminium on the 90° specimen, but our results show that this is not the case. Another point to consider is that the higher the pressure the higher the risk of creating microcracks and impair the entire surface.

One of the main disadvantages with aluminum contamination is that these areas with an added interface could give more stress to the material, where microfractures might start. Aluminium does not chemically bond to the cement either, therefore lowering the surface area it is able to bond to. The extra interface, that is only mechanically retained to the zirconia surface, could behave differently after several years with wear. Meaning that the aluminum contamination could have a more significant effect after cyclic loading.

4.3 Surface energy

Our results showed that the polar part of the surface energy on the unprimed specimen was lower than expected, compared to other studies. (31) (32) (33) This might be because of the contamination from hydrocarbons, as we can see on our contamination chart (Table 6) that around 5 wt.% of the surface is carbon. This is airborne carbon, that has reacted with the hydroxyl group on the zirconia surface. This will probably affect the priming as well, because the 10-MDP that reacts with the hydroxyl group will then have fewer vacant spots for attachment. The study from Al-Akhali (33) shows that surface free energy decreased significantly within 24 hours after airborne-particle abrasion, suggesting that zirconia restorations should be sandblasted as close to the cementation as possible because of the contamination from hydrocarbons and their influence on the zirconia surface. Our results support this, where we measured lower contact angles immediately after chemical cleaning. This suggests that chemical cleaning of the zirconia could be as effective as mechanical cleaning (APA) in removing contamination of hydrocarbons. Furthermore, chemical cleaning can be performed without the micromechanical damage from alumina-particles disturbing the surface at a high pressure.

Glycerol was intended to be used as one of our liquids to measure surface free energy. Because of its considerably higher viscosity compared to the other test liquids it was difficult to form proper droplets that would be comparable with the other liquids. All values from the contact angles were off the linear fit of the test array, and these measurements are therefore of little value in determining the apparent surface energy of the rough zirconia, and therefore omitted from the linear interpolation.

The glycerol contact angles were still measured on the non-primed specimen, as it is interesting to observe the effect of increased viscosity and how that behaves on the different surfaces. The cements usually have quite high viscosity, and glycerol is somewhat comparable to the cement in this matter. When the contact angles measured with glycerol were plotted for the surface energy calculation, these values were consistently below the values expected from the linear fit for the four test liquids used in this study. This implies that higher contact angle values were measured for zirconia than expected based on its surface energy. This can be explained by the roughness of the test surfaces, as higher force is generally needed to wet a surface with high viscosity fluid than a fluid with low viscosity and similar surface energy. (34) This discrepancy in wetting behavior becomes even more pronounced when the surface and the liquid have different surface energy components, as illustrated in Figure 3. The tested zirconia surface had low polar components and total surface energy (Table 4) and allowed only partial wetting of the surface with glycerol with higher polar component and total surface energy.

Comparing the anterior and posterior zirconia, the differences in surface free energy are small. However, we do see a clear difference between the untreated specimens. This might indicate that the surface of anterior zirconia is more affected by the APA than the posterior zirconia. The fact that the posterior zirconia already is stabilized in the tetragonal phase might be the reason why we do not see as many differences between the different groups on the posterior zirconia group. Since the results show that the treated zirconia materials behave very alike, there is no clear indication to treating the 2nd and 3rd generation differently. The treated anterior zirconia will probably "bind" the same way to the cement as the posterior zirconia.

Comparing the results of the surface energy of primed surfaces shows that the primers act quite alike. Clearfil Ceramic has a somewhat lower surface energy compared to the other primers. The non-silane primer (Z-prime) acts very similar to the Monobond (which contains silane). This gives us an indication that the silane is not affecting the surface energy of the primed surface, and we therefore suggest that the silane-containing primers could be used with the same cements as the non-silane primers. It is important to further investigate the effect of the silane as well. In a meta-analysis of bonding to zirconia (16), a main point in the discussion is the difference between non-silane vs silane primers. It is mentioned here that there are not enough studies showing if silane has a synergistic effect or a counteracting effect. Our results show no difference between the silane and no silane primers, suggesting that the silane does not affect the surface energy. None the less more studies on the bonding effect will be needed.

Many of the results with Anterior APA 45° 0,5 bar seem like outliers, behaving differently than is to be expected with the trend we see with increased pressure. If we look at the 3D-topography illustrations, we notice the grooves from the machining process almost unchanged to the control. A reason the discrepant wetting behavior on these samples could be a capillary effect that "pulls" and disperses the droplets to having a lower contact angle. The discs without these areas filled with deep grooves, will not have this effect, and give us a droplet with higher contact angle. The same principle is used when making zirconia implants, where microgrooves make the implants more hydrophilic to optimize the osseointegration. (35) This could be the explanation for the big variation of contact angle results we got in this specimen group that resulted in a surface free energy, on non-primed specimens, that looks like an outlier in Figure 7.

4.4 Surface roughness

Figure 13 consists of two images of the same spot with different imaging settings to show why we did not see the grooves on the control surface in the regular BSE images (Figure 12). BSE signal typically comes from 0.5-1 µm depth on the surface and is not very sensitive to surface topography. Switching off one of the detector panels in the electron microscope gave us more detail regarding the surface

topography and we could visualise the grooves on the control surface also with SEM. In addition to the microgrooved pattern, the higher resolution of SEM revealed the presence of large amount of ZrO2 debris from the polishing sintered on the surface, which further contributed to the high surface roughness values of the control samples.

There is no indication that the APA angle has a significant impact on the surface properties between the same pressure. Our results indicate that the angle does not change the roughness on the anterior discs. The results in the posterior discs indicate a statistically greater difference than would be expected by chance with 1 bar pressure, between APA 45° and 90°. However, we do not have a significant sample size to exclude outliers and need therefore more tests to conclude if this is a real significant difference. What we do see represented in Figure 6 is a trend of increased roughness with increased pressure, at least for the posterior discs, and somewhat for the anterior discs. We also see a difference between the control groups and the treated groups.

Statistically there is no difference in surface roughness between the anterior and posterior discs. With this, we conclude that crowns after sandblasting treatment (APA) should be treated the same in terms of roughness.

4.5 Sources of error

The cutting method must resemble the crown production process, here we have cut the discs mechanically which gave them a very rough surface compared to after the sintering process.

There is a need to test the surface free energy right after APA, to see the real effect if not right before cementation, since these measurements were made weeks after surface treatment.

5. Conclusions

Interestingly the results show differences in the surface energy of the anterior and posterior zirconia when the surface is untreated with APA. When the surface is treated, the anterior and posterior zirconia have almost identical surface free energy values. Suggesting that these materials can be treated the same way, even though they are completely different when untreated.

Our results do not tell us how much the fouling of the surface influences the effect of the primer. The different primers do behave very alike, and the silane content does not affect the surface free energy according to our results.

When the zirconia surfaces are treated with air particle abrasion, the surface will be contaminated by alumina. When sandblasting at 2 bar pressure, the contamination is significantly higher than at 1 and 0,5 bar pressure. In this study a tendency can be seen as a slope in the bars in the graph in Figure 6, more pronounced to the posterior group, where increased pressure tends to increase the aluminum content concentration (wt.%) on the zirconia surface after APA.

There is a significant contamination of the zirconia coins from airborne hydrocarbons as well. It could therefore be interesting to compare the results with newly APA treated surfaces, to determine the effect of the contamination on the surface free energy right before cementation. What we concluded with this study is that there is a need to either mechanically or chemically clean the zirconia surface after APA.

The surface roughness measurement (Sa) only tells us the average height deviation. This parameter does not explain the surface texture. In the illustrations of surface texture, we see that APA mostly eliminates the machined pattern and the highest peaks, where the patterns are almost no longer recognizable in the 2 bar imaging. The surface texture must also be considered for further research, for example in the effects on bonding between zirconia and cement.

5.1 Clinical implication

The two versions of Zirconia do behave very alike and can be treated the same way after APA. The angle used when APA, does not affect the roughness or the surface free energy. This means that the surface roughness and energy is not different inside the crown where an angle of 90° is not always possible to achieve.

Chemical cleaning of zirconia should be considered as a good option, as it is a gentler cleaning method to the surface compared to mechanical cleaning and have the same effect. Either way, some sort of mechanical or chemical cleaning is needed before cementation of the crown to remove hydrocarbon contamination.

Since these parameters have only been tested in vitro we will not be able to determine if these minimal differences have an effect in total for the retention and lifetime of a zirconia crown that has been cemented inside a patient's mouth, or the failure rate after wear.

6. Acknowledgements

We acknowledge Yann Dumay and Alejandro Barrantes for their assistance with surface roughness measurements.

7. References

1. **J, Hjerppe, P, Steyern and Vult, Von.** Two decades of zirconia as a dental biomaterial – what have we learned? *Tidende.* 1, 2019.
2. **Andersen, Freya S and Ruud, Amund.** Multilagszirkonia – optiske og mekaniske egenskaper. *Tidende.* 5, 2022.
3. **Guzzato, M, et al.** Strength, fracture toughness and microstructure of a selection of all-ceramic materials. Part II. Zirconia-based dental ceramics. *Dent Mater.* 20, 2004.
4. **Bocanegra-Bernal, M. H. and Diaz, Sebastián.** Phase transitions in zirconium dioxide and related materials for high performance engineering ceramics. *Journal of Materials Science.* 37, 2002.
5. **Mihai, Laurenta Lelia, et al.** In vitro Study of the Effectiveness to Fractures of the AestheticFixed Restorations Achieved from Zirconium and Alumina. *Revista de Chemie.* 65, 2014.
6. **J, Chevalier, et al.** The Tetragonal-Monoclinic Transformation in Zirconia: Lessons Learned and Future Trends. J Am Ceram Soc. 2009;92(9):1901-20. *J Am Ceram Soc.* 92, 2009.
7. **Reisegg, Kjetil, Schriwer, Christian and Øilo, Marit.** Zirkonia som dentalt keram. *Tidende.* 4, 2017.
8. **Zhang, Y and Lawn, BR.** Novel Zirconia Materials in Dentistry. *Journal of Dental Reaserch.* 2, 2018.
9. **Kawai, Yohei, et al.** Phase transformation of zirconia ceramics by hydrothermal degradation. *Dent Mater J.* 30, 2011, 3.
10. **Tong, Hui, et al.** Characterization of three commercial Y-TZP ceramics produced for their high-translucency, high-strength and high-surface area. *Ceram Int.* Jan 1, 2016, pp. 1077-1085.
11. **Baldissara, Paolo, et al.** Translucency of IPS e.max and cubic zirconia monolithic crowns. *The Journal of Prosthetic Dentistry.* 2, 2018, 120.
12. **Zhang, F, et al.** Strength, toughness and aging stability of highly-translucent Y-TZP ceramics for dental restorations. *Dent MAter.* 32, 2016.
13. **N., Cavalcanti A., et al.** Bond Strength of Resin Cements to a Zirconia Ceramic with Different Surface Treatments. *Oper Dent.* 3, 2009, 34.
14. **Fu, Le, Engqvist, Håkan and Xia, Wei.** Glass-Ceramics in Dentistry: A Review. *Materials.* 5, 2020, 13.
15. **Nagaoka, Noriyuki, et al.** Chemical interaction mechanism of 10-MDP with zirconia. *Scientific Reports.* 7, 2017.
16. **Inokoshi, M, et al.** Meta-analysis of bonding effectiveness to zirconia ceramics. *J Dent Res.* 4, 2014.
17. **[Online] [Cited: 05 12, 2022.] https://curion.ca/products/z-prime-plus.**

18. **[Online] [Cited: 05 12, 2022.] https://www.kuraraynoritake.eu/en/clearfil-universal-bond-quick .**
19. **[Online] [Cited: 05 12, 2022.] https://www.ivoclar.com/en_in/products/cementation/monobond-plus.**
20. **Hansen, Nadine Anika, Wille, Sebastian and Kern, Matthias.** Effect of reduced airborne-particle abrasion pressure on the retention of zirconia copings resin bonded to titanium abutments. *J Prosthet Dent.* 2020.
21. **Øilo, Marit and Schriwer, Christian.** Dentale keramer - estetikk og klinisk anvendelse. *Tidende.* 5, 2017.
22. **Kuznetsova, T, et al.** Evaluation of adhesive forces and the specific surface energy of zirconia stabilized by yttria with alumina additions ceramic by AFM method. *Methodological aspects of scanning probe microscopy strony* . 1, 2016.
23. **Wikipedia.** Surface energy. *Wikipedia.* [Online] December 12, 2021. [Cited: May 19, 2022.] https://en.wikipedia.org/wiki/Surface_energy.
24. **Wendt , R.C. and Owens ,** D.K. Estimation of the surface free energy of polymers. *Journal of Applied Polymer Science.* 1969, Vol. 13, 1741.
25. **DataPhysics Instruments GmbH.** DataPhysics Understanding Interfaces. *Contact angle.* [Online] [Cited: april 18, 2022.] https://www.dataphysics-instruments.com/knowledge/understanding-interfaces/contact-angle/.
26. **—. DataPhysics Understanding Interfaces.** *Dispersive & polar parts of the surface energy and surface tension.* [Online] [Cited: april 19, 2022.] https://www.dataphysics-instruments.com/knowledge/understanding-interfaces/dispersive-polar-parts/.
27. **—. DataPhysics Understanding Interfaces.** *Determination of the surface energy of a solid.* [Online] [Cited: april 18, 2022.] https://www.dataphysics-instruments.com/knowledge/understanding-interfaces/solid-surface-energy/.
28. **Bonola, C, et al.** Luminescence of defect centres in electroreduced single crystals of yttria-stabilized zirconia. *Journal of Luminescence.* 48-49, 1991, 2.
29. **Sinhamahapatra, Apurba, et al.** Oxygen-Deficient Zirconia (ZrO2−x): A New Material for Solar Light Absorption. *Scientific Reports.* 6, 2016.
30. **Camposilvan, E, et al.** Aging resistance, mechanical properties and translucency of different yttria-stabilized zirconia ceramics for monolithic dental crown applications. *Dental Materials.* 6, 2018.
31. **Ishii, Ryo, et al.** Influence of surface treatment of contaminated zirconia on surface free energy and resin cement bonding. *Dental Materials Journal.* 34, 2015, 1.
32. **Akazawa, Nobutaka, et al.** Effect of etching with potassium hydrogen difluoride and ammonium hydrogen difluoride on bonding of a tri-n-butylborane initiated resin to zirconia. *Dental Materials Journal.* 38, 2018, 4.
33. **Al-Akhali, Majed, et al.** Influence of elapsed time between airborne-particle abrasion and bonding to zirconia bond strength. *Dental Materials.* 3, 2021.
34. **Courbin, L, et al.** Dynamics of wetting: from inertial spreading to viscous imbibition. *Journal of Physics: Condensed Matter.* 21, 2009, 46.
35. **Dantas, T. A., et al.** Design and optimization of zirconia functional surfaces for dental implants applications. *Ceramics International.* 46, 2020, 10.
36. **UiO Institute of Clinical Dentistry. Odont.uio.** ***Biomaterials Capacities: Tabletop Microscope (SEM).*** **[Online] https://www.odont.uio.no/iko/english/about/organization/units/biomaterials/Capacities/tabletop-microscope/.**
37. **—. Odont.uio.** ***Biomaterials Capacities: UV/ozone cleaner.*** **[Online] December 7, 2018. [Cited: april 21, 2022.] https://www.odont.uio.no/iko/english/about/organization/units/biomaterials/Capacities/uvo-cleaner/.**

8. Appendix